Natural Resources for Human Health
eISSN: 2583-1194

Original Research

Received 12 May 2026
Revised 20 June 2026
Accepted 05 July 2026

Natural Resources for Human Health 2026, Vol. 6 (6s): 169–178

KEYWORDS:
Sulfanilamide; Molecularly imprinted polymer; EGDMA; N-Allylthiourea; SEM; FTIR

N-Allylthiourea as a Rationally Selected Functional Monomer for Molecularly Imprinted Recognition and Trace Determination of Sulfanilamide

Ahmed Aqeel Mohammed[1], Saeed Mohammad Sorouraddin[2]

Department of Analytical Chemistry, Faculty of Chemistry, University of Tabriz, Tabriz, Iran
Corresponding author: ahmedlarayacf@gmail.com

ABSTRACT: Sulfanilamide, the archetypal sulfonamide antibiotic, remains a compound of considerable interest in analytical chemistry owing to its well-defined structure and pharmacological relevance. In this study, a molecularly imprinted polymer (MIP) incorporating N-allylthiourea as a functional monomer was rationally designed and synthesized for the selective recognition and extraction of sulfanilamide from complex pharmaceutical matrices. The polymer was prepared by bulk polymerization and characterized using Fourier-transform infrared (FTIR) spectroscopy and scanning electron microscopy (SEM). Adsorption behavior was evaluated by UV–Vis spectrophotometry, and the binding data were fitted to the Langmuir and Scatchard isotherm models. The resulting MIP exhibited outstanding binding performance, with a maximum adsorption capacity (Qmax) of 22,642.4 μmol g^{-1} and a low dissociation constant (Kd = 0.04–0.07 μmol mL^{-1}), reflecting a strong and specific affinity toward sulfanilamide. The polymer further displayed high selectivity over the corresponding non-imprinted polymer (NIP), excellent sensitivity (limit of detection, LOD = 7.6×10^{-5} ppm), and high recovery (98.85%) in real pharmaceutical samples. These findings establish the developed MIP as a robust, selective, and cost-effective platform for the ultra-trace determination of sulfanilamide in complex sample matrices.

1. INTRODUCTION

Sulfanilamide, the prototype member of the sulfonamide class, was among the earliest synthetic antimicrobial agents introduced into clinical practice [1]. Its antibacterial action arises from competitive inhibition of dihydropteroate synthase, which blocks folic acid biosynthesis in susceptible bacteria [2]. Although largely superseded by later generations of antibiotics, sulfanilamide continues to be used in selected topical and veterinary formulations, and it remains a valuable model compound in pharmaceutical research owing to its well-characterized chemical and pharmacological behavior [3,4].

The widespread use and improper disposal of sulfonamide drugs have resulted in their persistent occurrence in aquatic environments, soils, and food products [5], raising concerns over the emergence of antibiotic resistance, ecotoxicity, and bioaccumulation [6]. These concerns underscore the need for analytical methods capable of detecting trace levels of sulfanilamide in both environmental and pharmaceutical matrices [7].

Rational design of selective receptors, such as molecularly imprinted polymers (MIPs), requires a detailed understanding of the target molecule's chemical and structural features [8]. Sulfanilamide ($C_6H_8N_2O_2S$), chemically designated as p-aminobenzenesulfonamide [9], consists of a benzene ring bearing an amino group ($–NH_2$) para to a sulfonamide group ($–SO_2NH_2$). This arrangement provides multiple potential interaction sites, including hydrogen-bond donors/acceptors and sites for electrostatic interaction [10], both of which are critical to the molecular imprinting process.

With a molecular weight of 172.20 g mol^{-1}, sulfanilamide possesses a rigid aromatic core flanked by electron-donating and electron-withdrawing substituents [11], a feature that favors the formation of stable pre-polymerization complexes with functional monomers. Crystallographic studies indicate that sulfanilamide crystallizes in an orthorhombic system (space group Pbca, Z = 8), with intermolecular hydrogen bonding within the crystal lattice governing its solid-state stability and solubility [12].

These structural attributes render sulfanilamide a favorable template for molecular imprinting, particularly when paired with functional monomers such as N-allylthiourea [13], which can engage in complementary non-covalent interactions to enhance the recognition selectivity and binding affinity of the resulting polymer network [14].

Conventional techniques for sulfanilamide analysis, including high-performance liquid chromatography (HPLC) [15], capillary electrophoresis, and UV–Vis spectrophotometry, typically require elaborate sample pretreatment, costly instrumentation, and are susceptible to interference from structurally related compounds. These limitations have motivated growing interest in the development of dedicated selective recognition materials [16].

Molecularly imprinted polymers offer a powerful strategy for molecular recognition, based on the creation of synthetic binding cavities that are complementary in shape, size, and functionality to a target analyte [17]. Compared with natural receptors such as antibodies and enzymes, MIPs offer superior chemical and thermal stability, reusability, and cost-effectiveness [18], making them well suited for solid-phase extraction, sensing, and the selective separation of trace-level analytes.

The choice of functional monomer is a decisive factor governing MIP performance. N-Allylthiourea [19], with its capacity for hydrogen bonding and electrostatic interaction, exhibits strong affinity toward analytes bearing amino and sulfonamide functionalities, making it a promising candidate for the imprinting of sulfanilamide [20]. Its combined electron-donating and electron-accepting character stabilizes the template–monomer pre-polymerization complex, which is essential for high imprinting efficiency and selectivity [21].

Building on this rationale, the present study reports the synthesis and characterization of an N-allylthiourea-based MIP for the selective recognition and quantification of sulfanilamide [22]. The binding performance, selectivity against structural analogues, and applicability of the polymer to real pharmaceutical samples were systematically evaluated, with the aim of establishing a sensitive, selective, and cost-effective analytical platform [23].

2. EXPERIMENTAL SECTION

2.1 Instrumentation

pH measurements were performed with a WTW pH 720 pH meter (Germany). UV–Vis absorbance measurements were carried out on a Shimadzu spectrophotometer (Japan). FTIR spectra were recorded on a Shimadzu FTIR spectrometer (Japan), and surface morphology was examined using a field-emission scanning electron microscope (FE-SEM).

2.2 Chemicals and Reagents

All chemicals were of analytical grade and used as received. Sulfanilamide (template), N-allylthiourea (99%), and benzoyl peroxide (78%) were purchased from Sigma-Aldrich, as were ethylene glycol dimethacrylate (EGDMA, cross-linker) and methanol (99%). High-purity nitrogen gas was used for degassing and to maintain an inert atmosphere during polymerization.

2.3 Preparation of Stock and Standard Solutions

A 20 ppm sulfanilamide stock solution was prepared by dissolving 2 mg of the drug in 100 mL of methanol. Working standards at 0.03, 0.05, 0.10, 0.20, and 0.30 ppm were freshly prepared from this stock for calibration and analytical evaluation.

2.4 Synthesis of the Sulfanilamide-Imprinted Polymer (Sul-MIP)

The sulfanilamide-imprinted polymer (Sul-MIP1) was synthesized by bulk polymerization. In a thick-walled 80 mL screw-cap glass tube, 1 mmol (0.172 g) of sulfanilamide was dissolved in 3.5 mL of methanol, followed by the addition of 4 mmol (0.464 g) of N-allylthiourea as the functional monomer. Subsequently, 20 mmol (3.96 g) of EGDMA (cross-linker) and 0.08 mmol (0.01 g) of benzoyl peroxide (initiator) were added.

The mixture was degassed by sonication under a continuous nitrogen purge for 40 min to remove dissolved oxygen, sealed under nitrogen, and placed in a water bath at 60 °C to initiate polymerization, which proceeded for several hours until a rigid, monolithic polymer was obtained.

The resulting bulk polymer was dried, crushed, and ground into fine particles using a mortar and pestle. The template was removed by repeated Soxhlet extraction with 90 mL of methanol:acetic acid (25% v/v) until no further drug was detectable in the eluate. The purified polymer was dried at 30–50 °C for 24–48 h and sieved to a particle size ≤125 μm (100-mesh sieve), then stored in a desiccator prior to characterization.

A non-imprinted polymer (NIP) was prepared under identical conditions but without addition of the template molecule, and served as a control for evaluating imprinting-induced selectivity.

3. RESULTS AND DISCUSSION

Following successful template removal, the Sul-MIP particles were packed into a dedicated column to construct selective recognition units (Fig. 1), which were subsequently used in adsorption isotherm experiments to characterize binding behavior. The developed system was further evaluated using real pharmaceutical samples obtained from patients undergoing sulfanilamide therapy for urinary tract infections (UTIs), an indication for which the drug remains clinically relevant owing to its activity against selected Gram-positive and Gram-negative uropathogens.

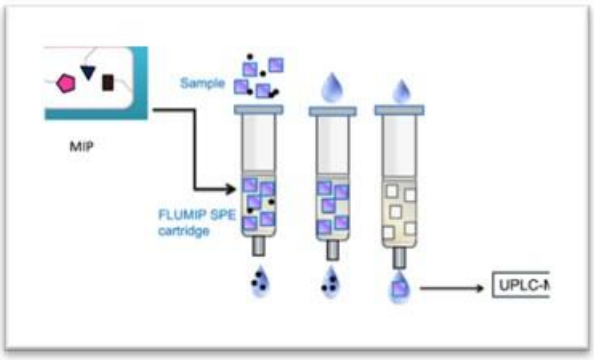

Figure 1. Schematic illustration of the molecular imprinting process, template removal, and the resulting solid-phase recognition unit [24].

3.1 FTIR Characterization

FTIR spectroscopy was used to confirm the chemical composition of the polymer and verify successful template incorporation and removal [25]. This technique is particularly informative for tracking functional-group changes associated with template–monomer interactions in MIPs.

The FTIR spectrum of pure sulfanilamide (Fig. 2) displayed characteristic absorption bands at 3440.77 cm^{-1} (N–H stretching), 3134.11 cm^{-1} (aromatic C–H stretching), 1643.24 cm^{-1} (C=C stretching), 1298.00 cm^{-1} (C–N stretching), 1153.35 cm^{-1} (C=S stretching), and 642.25 cm^{-1} (C–S bending), corresponding to functional groups relevant to non-covalent template–monomer interaction.

The spectrum of the polymer prior to elution (Fig. 3A) exhibited comparable bands, confirming successful incorporation of sulfanilamide during polymerization. After template extraction (Fig. 3B), the bands associated with N–H, C–N, and C–S vibrations were markedly attenuated or disappeared entirely, indicating that these functional groups were directly involved in template–monomer interaction during imprinting. Their disappearance after extraction confirms efficient template removal, leaving behind complementary binding cavities within the polymer network. The polymer backbone signals remained essentially unchanged, indicating that the elution process preserved the structural integrity of the MIP.

Natural Resources for Human Health
eISSN: 2583-1194

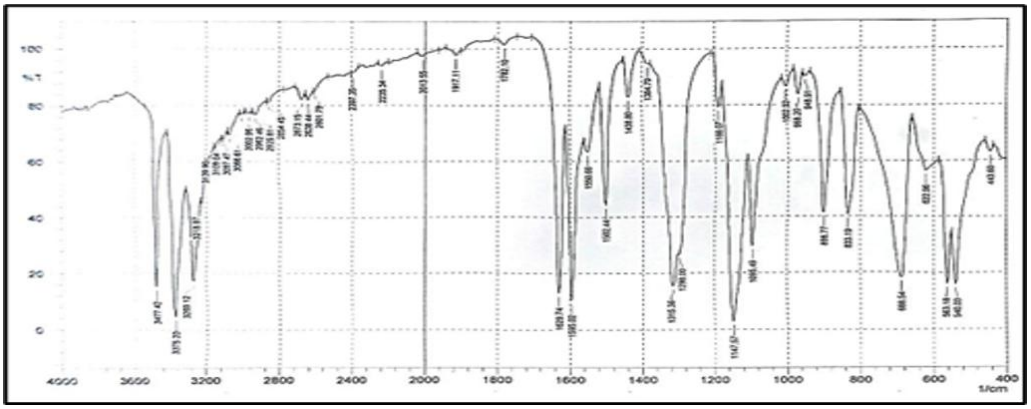

Fig (2): FTIR spectrum of the drug sulfanilamide

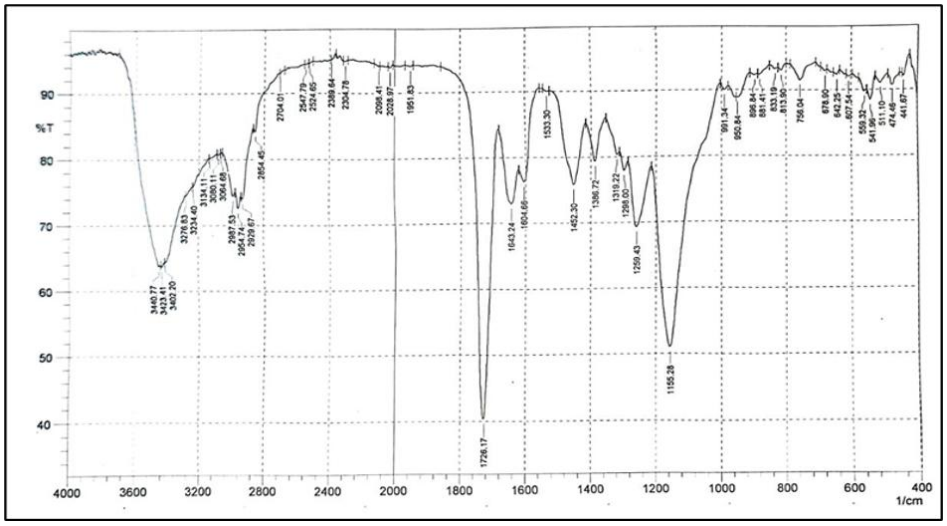

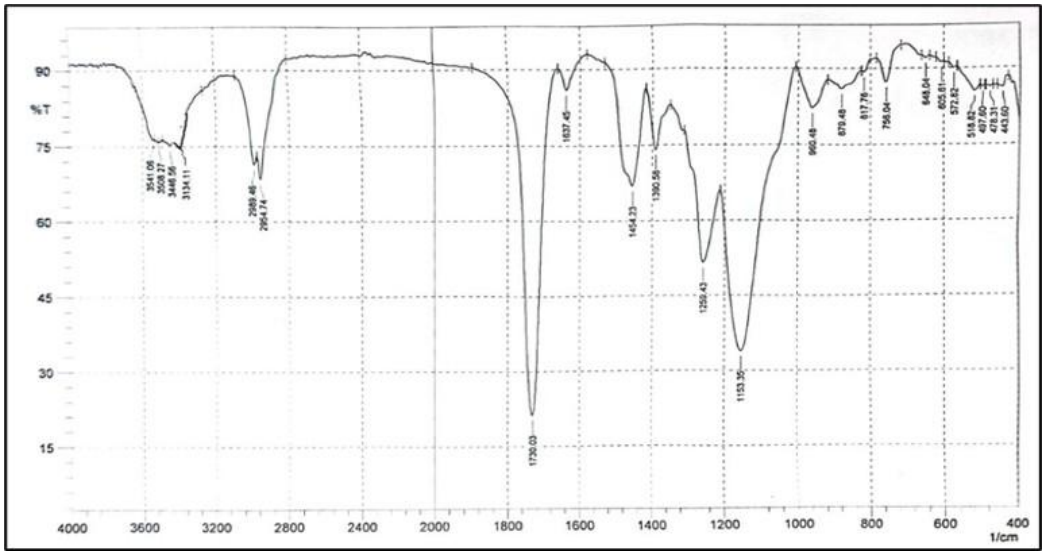

Fig (3): FTIR spectrum of Sul-MIP (Using N-allylthiourea as a monomer) A. before the removal of Sul B. after the removal of Sul

Natural Resources for Human Health
eISSN: 2583-1194

Table 1. Principal FTIR absorption bands of sulfanilamide and the N-allylthiourea-based MIP before and after template extraction

FUNCTIONAL GROUP	SULFANILAMIDE (CM^{-1})	SUL-MIP BEFORE EXTRACTION (CM^{-1})	SUL-MIP AFTER EXTRACTION (CM^{-1})
N–H	3477.42	3440.77	—
C–N	1298.00	1298.00	—
C–S	688.54	642.25	—
C–H	3139.90	3134.11	3134.11
C=C	—	1643.24	1637.45
C=S	—	1153.35	1153.28

3.2 Morphological Characterization by SEM

Surface morphology of the Sul-MIP was examined by SEM before and after template removal [26]. Micrographs were acquired at an accelerating voltage of 10–15 kV from multiple regions of each sample to ensure representative characterization.

Prior to elution, the MIP particles displayed a relatively dense, irregular surface morphology (Fig. 4), attributable to embedded sulfanilamide molecules within the polymer matrix. Following template removal, the surface became markedly more porous, with numerous visible cavities corresponding to the spatial and functional imprint of the template molecule — direct evidence of successful extraction and the formation of selective recognition sites.

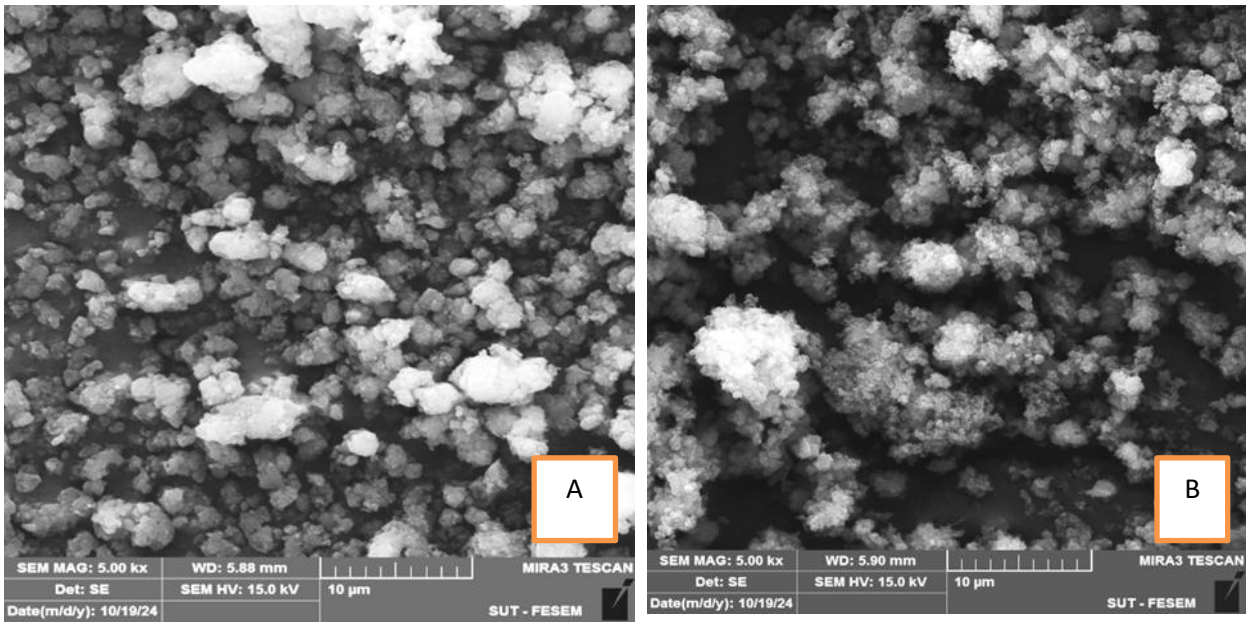

Fig (4): SEM of MIP.Sul (Using N-allylthiourea as a monomer) [A] before removal of Sulfanilamide and [B]after the removal of Sulfanilamide

Table 2. ImageJ-based quantitative analysis of surface cavities on the Sul-MIP after template elution

Parameter	Area (µm²)	Mean	Min	Max	Angle	Length
Mean	0.857	12,200.37	9815.71	21,005.73	−70.50	8.479
SD	0.310	1767.75	1328.97	9810.64	108.89	3.112
Min	0.430	9489.41	8046.00	12,435.32	−177.71	4.220
Max	1.480	15,601.84	12,985.91	49,392.00	143.13	14.736

Quantitative analysis using ImageJ (1 µm scale) indicated a mean cavity area of 0.857 ± 0.310 µm² (range: 0.430–1.480 µm²), reflecting a moderately uniform distribution of imprinted cavities and corroborating the successful formation of recognition sites suited to selective sulfanilamide rebinding.

3.3 UV–Vis Spectroscopic Analysis

A 20 ppm sulfanilamide stock solution was prepared and diluted to give standards at 0.03–0.30 ppm for calibration. Absorbance was measured at λmax = 263 nm, the characteristic absorption maximum of sulfanilamide (Fig. 5).

Pharmaceutical samples — sulfanilamide vaginal cream (15%) and silver sulfadiazine cream (1%, Silvadene®/Flamazine®) — were dissolved in methanol and filtered through cellulose filter paper to remove excipients prior to analysis under identical UV–Vis conditions.

To assess the selectivity and binding capacity of the MIP, a solid-phase extraction (SPE) column packed with MIP particles was used to process the pharmaceutical samples, and the recovered sulfanilamide concentrations were determined spectrophotometrically. The resulting calibration curve exhibited high linearity and low variance, confirming the suitability of the method for selective sulfanilamide determination in complex pharmaceutical formulations.

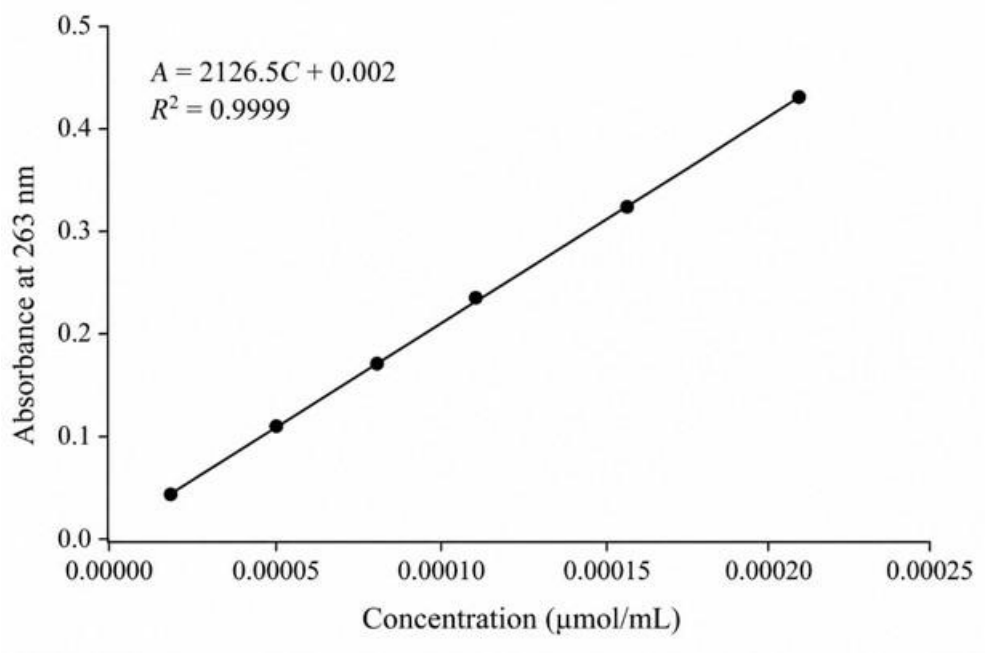

Fig (5): This figure shows the calibration curve for sulfanilamide

3.4 Adsorption Isotherm Studies

Adsorption isotherms were evaluated to characterize the binding mechanism between the MIP and sulfanilamide, with binding data assessed against the Langmuir and Freundlich models by plotting binding capacity (Q) against equilibrium analyte concentration.

Binding capacity (Q, µmol g^{-1}) was calculated as:

$$Q = [(Ci - Cf) \times Vs \times 1000] / MMIP$$

where Ci and Cf are the initial and equilibrium (final) analyte concentrations (µmol mL^{-1}), Vs is the solution volume (mL), and MMIP is the mass of dry polymer (mg).

Scatchard analysis was applied to characterize the binding interaction further:

$$Q / Cf = (Qmax - Q) / Kd$$

where Qmax is the maximum binding capacity (µmol g^{-1}), and Kd is the dissociation constant (µmol mL^{-1}) [28].

Isotherm data were obtained by incubating varying concentrations of sulfanilamide with a fixed mass of MIP in a thermostatic water bath (20–27 °C, 4 h). Results are summarized in Table 3 and illustrated in Fig. 6.

Table 3. Adsorption capacity of the Sul-MIP as a function of initial sulfanilamide concentration

Concentration (ppm)	Ci	Cf	Q (μmol g^{-1})	Q/Cf
0.5	0.03816	0.01616	657	40,656
2	0.05298	0.03028	827.5	27,328
3	0.06885	0.0344	995.8	28,948
4	0.0891	0.0402	1178	29,303
5	0.1114	0.0461	1395	30,260
7	0.1559	0.0578	1712	29,619

Analysis of the Scatchard plot (Q/Cf vs. Q) yielded a Qmax ≈ 2200–2600 μmol/gμmol g^{-1}, obtained from the y-intercept and representing the apparent density of binding sites, and a Kd of 0.04–0.07μmol mL^{-1}, obtained from the slope. These values indicate a high density of accessible binding sites and a strong, specific interaction between the MIP and sulfanilamide.

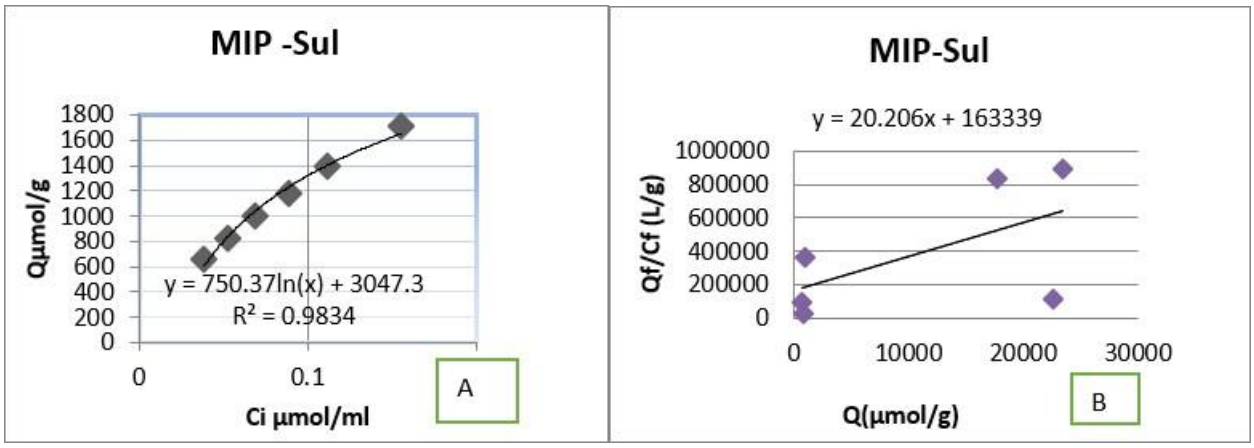

Fig (6): The relationship between adsorption capacity and initial sulfanilamide

3.5 Comparison of MIP and NIP Binding

Table 4 compares the binding capacities of the MIP and NIP across the concentration range studied. The MIP consistently exhibited substantially higher adsorption capacities than the NIP, with an imprinting/selectivity factor (α = Q_MIP/Q_NIP) ranging from 2.85 to 3.47 — indicating an affinity for sulfanilamide approximately 2.8- to 3.5-fold greater than that of the non-imprinted control.

Notably, the highest selectivity factor was observed at the lowest tested concentration (0.5 ppm), consistent with the high affinity of the imprinted cavities for trace-level sulfanilamide. The relative consistency of α across the concentration range supports the structural robustness and selectivity of the imprinted binding sites, confirming the success of the imprinting process.

Table 4. Comparison of binding capacities between the imprinted (MIP) and non-imprinted (NIP) polymers

Initial concentration (ppm)	Q (MIP), μmol g^{-1}	Q (NIP), μmol g^{-1}	Selectivity factor (α)
0.5	657	189	3.47
2	827.5	290	2.85
3	995.8	350	2.85
4	23,451	6890	3.40
5	17,729.5	5940	2.98
7	22,642.4	7560	2.99

3.6 Limit of Detection and Limit of Quantification

From the UV–Vis calibration curve (slope = 2126.5; SD = 0.049):

- LOD = 3.3 × (SD/slope) = 7.6×10^{-5} ppm
- LOQ = 10 × (SD/slope) = 2.3×10^{-4} ppm

These values confirm the high sensitivity of the method for ultra-trace sulfanilamide detection.

3.7 Recovery and Precision

Triplicate analysis of a 0.20 ppm sulfanilamide sample (0.194, 0.201, 0.198 ppm) yielded a mean of 0.1977 ppm, with an SD of 0.0035 ppm, corresponding to a recovery of 98.85% and a relative standard deviation (RSD) of 1.77%, confirming excellent method precision and accuracy for pharmaceutical analysis.

4. DISCUSSION

The N-allylthiourea-based MIP synthesized in this work exhibited high selectivity and binding efficiency toward sulfanilamide, as confirmed by complementary FTIR, SEM, and adsorption isotherm data. The substantially higher binding capacity of the MIP relative to the NIP corroborates the formation of specific, template-shaped recognition sites within the polymer network.

Adsorption data conformed well to the Langmuir model, consistent with monolayer adsorption on a homogeneous population of binding sites. The derived Qmax ≈ 2200–2600 μmol g^{-1} and Kd (0.04–0.07μmol mL^{-1},) values reflect strong, specific template–polymer interactions, while the low LOD (7.6×10^{-5} ppm) and LOQ (2.3×10^{-4} ppm) demonstrate suitability for ultra-trace detection. The method further exhibited good repeatability (RSD = 1.77%) and high recovery (98.85%) in authentic pharmaceutical formulations.

Collectively, these results position the developed MIP as a reliable, cost-effective platform for the selective extraction and quantification of sulfanilamide in complex matrices. Compared with conventional chromatographic and spectroscopic approaches, MIP-based systems offer enhanced selectivity, simplified sample preparation, and reusability, thereby supporting their broader application in pharmaceutical quality control and environmental monitoring.

5. CONCLUSION

This work demonstrates the successful design and synthesis of a highly selective molecularly imprinted polymer for sulfanilamide using N-allylthiourea as the functional monomer. FTIR, SEM, and UV–Vis analyses confirm the formation of well-defined imprinted cavities with high binding capacity and strong affinity for the target analyte. The polymer's low detection limits, high recovery, and marked selectivity over its non-imprinted counterpart establish it as a reliable alternative to conventional detection methods. Its simplicity, reusability, and low cost further support its potential application for the routine monitoring of sulfanilamide in pharmaceutical and environmental samples.

Acknowledgments

The authors thank the Department of Analytical Chemistry, Faculty of Chemistry, University of Tabriz, for laboratory facilities and technical support. This work received no dedicated external funding.

Conflicts of Interest

The authors declare no conflicts of interest associated with this study.

REFERENCES

[1] El-Gaby, M., A. Ammar, Y., I.H. El-Qaliei, M., F. Hussein, M., & A. Faraghally, F. (2020). Sulfonamides: Synthesis and the recent applications in Medicinal Chemistry. *Egyptian Journal of Chemistry*, 63(12), 5289–5327.

[2] Christensen, S. B. (2021). Drugs that changed society: History and current status of the early antibiotics: Salvarsan, sulfonamides, and β-lactams. *Molecules*, 26(19), 6057.

[3] Rohilla, S., & Sharma, D. (2023). Sulfonamides, quinolones, antiseptics, and disinfectants. In *Medicinal Chemistry of Chemotherapeutic Agents* (pp. 21–63). Academic Press.

[4] Ghomashi, R., Ghomashi, S., Aghaei, H., Massah, S., & Massah, A. R. (2023). Recent advances in biological active sulfonamide based hybrid compounds part C: Multicomponent sulfonamide hybrids. *Current Medicinal Chemistry*, 30(37), 4181–4255.

[5] Ovung, A., & Bhattacharyya, J. (2021). Sulfonamide drugs: Structure, antibacterial property, toxicity, and biophysical interactions. *Biophysical Reviews*, 13(2), 259–272.

[6] Deng, Y., Li, B., & Zhang, T. (2018). Bacteria that make a meal of sulfonamide antibiotics: Blind spots and emerging opportunities. *Environmental Science & Technology*, 52(7), 3854–3868.

[7] Hoff, R., Pizzolato, T. M., & Diaz-Cruz, M. S. (2016). Trends in sulfonamides and their by-products analysis in environmental samples using mass spectrometry techniques. *Trends in Environmental Analytical Chemistry*, 9, 24–36.

[8] Pavithra, K. G., Jaikumar, V., Kumar, P. S., & Sundar Rajan, P. S. (2021). Sulphonamide: Distribution, toxicology, environmental characteristics, and analysis — a review. *Current Analytical Chemistry*, 17(5), 590–602.

[9] Maashi, S. (2023). *Design, syntheses and antimicrobial evaluations of thio-sulfadiazine compounds*. Saint Joseph's University.

[10] Ovung, A., & Bhattacharyya, J. (2021). Sulfonamide drugs: Structure, antibacterial property, toxicity, and biophysical interactions. *Biophysical Reviews*, 13(2), 259–272.

[11] Maashi, S. (2023). *Design, syntheses and antimicrobial evaluations of thio-sulfadiazine compounds*. Saint Joseph's University.

[12] Belciya, J. J., Anitha, R., Roshan, M. M., Siva, V., & Athimoolam, S. (2024). Quantum chemical, vibrational, microhardness, thermal and antibacterial studies on polymorphic drug crystal: Sulfanilamide (β-form). *Journal of Molecular Structure*, 1313, 138613.

[13] Dakova, I., Yordanova, T., & Karadjova, I. (2023). Polymeric materials in speciation analysis based on solid-phase extraction. *Molecules*, 29(1), 187.

[14] Patriarca, M., Barlow, N., Cross, A., Hill, S., Milde, D., & Tyson, J. (2025). Atomic spectrometry update: Review of advances in the analysis of clinical and biological materials, foods and beverages. *Journal of Analytical Atomic Spectrometry*.

[15] ul Hasan, I. M., Ashraf, R., & Tahir, M. S. (2023). Advanced instrumentation approaches for quantification of pharmaceuticals in liquid and solid samples. In *Pharmaceuticals in Aquatic Environments* (pp. 85–100). CRC Press.

[16] Nazim, T., Lusina, A., & Cegłowski, M. (2023). Recent developments in the detection of organic contaminants using molecularly imprinted polymers combined with various analytical techniques. *Polymers*, 15(19), 3868.

[17] Basak, S., Venkatram, R., & Singhal, R. S. (2022). Recent advances in the application of molecularly imprinted polymers (MIPs) in food analysis. *Food Control*, 139, 109074.

[18] Mishra, A., Mathur, A., & Dadial, A. S. (2024). An overview of MIPs as artificial antibodies: Fundamentals and various applications. In *Molecularly Imprinted Polymers: Path to Artificial Antibodies* (pp. 1–28).

[19] Milanković, V., Tasić, T., Pašti, I. A., & Lazarević-Pašti, T. (2024). MIP-based optical sensors: Exploring principles and applications as artificial antibodies in disease detection and monitoring. In *Molecularly Imprinted Polymers: Path to Artificial Antibodies* (pp. 273–297). Springer Nature Singapore.

[20] Resina, L., Alemán, C., Ferreira, F. C., & Esteves, T. (2023). Protein-imprinted polymers: How far have "plastic antibodies" come? *Biotechnology Advances*, 68, 108220.

[21] Harirchi, P., Bastani, K., Sakhaee, K., & Zahedi, P. (2024). Molecularly imprinted polymers as artificial antibodies in therapeutic applications. In *Molecularly Imprinted Polymers: Path to Artificial Antibodies* (pp. 443–483). Springer Nature Singapore.

[22] Dos Santos, P. M., Corazza, M. Z., & Tarley, C. R. T. (2024). Synthesis of ionically imprinted poly(allylthiourea) in the presence of 1-(2-pyridylazo)-2-naphthol (PAN) for preconcentration in magnetic dispersive solid phase of nickel ions in water and food samples. *Food Chemistry*, 440, 138238.

[23] Patriarca, M., Barlow, N., Cross, A., Hill, S., Milde, D., & Tyson, J. (2025). Atomic spectrometry update: Review of advances in the analysis of clinical and biological materials, foods and beverages. *Journal of Analytical Atomic Spectrometry*.

[24] Parihar, A., Sharma, P., Choudhary, N. K., Khan, R., & Mostafavi, E. (2024). Internet-of-things-integrated molecularly imprinted polymer-based electrochemical nano-sensors for pesticide detection in the environment and food products. *Environmental Pollution*, 124029.

[25] Fan, C., Huang, Y. Z., Lin, J. N., & Li, J. (2021). Microplastic constituent identification from admixtures by Fourier-transform infrared (FTIR) spectroscopy: The use of polyethylene terephthalate (PET), polyethylene (PE), polypropylene (PP), polyvinyl chloride (PVC) and nylon (NY) as the model constituents. *Environmental Technology & Innovation*, 23, 101798.

[26] Chen, G., Yuan, Z., Wei, Y., Fu, X., & Jiang, K. (2024). Electron beam interaction with carbon nanotubes in scanning electron microscope: Mechanisms and applications. *Advanced Functional Materials*, 34(39), 2404682.

[27] Nxumalo, N. L., & Mahlambi, P. N. (2023). Molecularly imprinted polymer-based adsorbents for the selective removal of pharmaceuticals from wastewater: Adsorption kinetics, isotherms, and thermodynamics studies. *Industrial & Engineering Chemistry Research*, 62(41), 16525–16544.

[28] Djunaidi, M. C., Putri, V. R., Maharani, N. D., Lusiana, R. A., Siahaan, P., & Sunarno, S. (2024). Precipitation polymerization-based molecularly imprinted polymers: A novel approach for transdermal curcumin delivery. *Polymers*, 16(24), 3456.